Hexagonal two layers-photonics crystal fiber based on surface plasmon resonance with gold coating biosensor easy to fabricate

Dedi Irawan[1], Khaikal Ramadhan[2], Saktioto[2], Fitmawati[3], Dwi Hanto[4], Bambang Widyatmoko[4]

[1]Department of Physics Education, University Riau, Pekanbaru, Indonesia
[2]Department of Physics, University Riau, Pekanbaru, Indonesia
[3]Department of Biology, University Riau, Pekanbaru, Indonesia
[4]Research Center of Physics, National Research and Innovation Agency (PUSPIPTEK), South Tangerang, Indonesia

Article Info

ABSTRACT

In this paper, we investigate a hexagonal two-layer photonic crystal fiber based on surface plasmon resonance (HT-PCF-SPR) which is easy to fabricate as a sensor for detecting the refractive index of analytes. After performing numerical simulations using COMSOL multiphysics based on the finite element method (FEM), it was found that the HT-PCF-SPR could detect the analyte's refractive index in the range 1.34-1.37 RIU and in the wavelength range from 730 nm to 810 nm. The plasmonic material used in the design is gold with a thickness of 40 nm which is located outside the layer and in two opposite air holes in the core. The HT-PCF-SPR design has good performance in detecting analytes, it is found that the sensitivity in detecting analytes is 2,000 nm/RIU, meaning that every 1 RIU shift of analyte shifts the wavelength by 2000 nm. Meanwhile, the sensor resolution obtained from the design is 6.67×10^{-5} RIU, and it is found that the larger the air hole, the greater the confinement loss value.

Corresponding Author:

Dedi Irawan
Department Physics Education, University Riau
Pekanbaru, Indonesia
Email: dedi.irawan@lecturer.unri.ac.id

1. INTRODUCTION

In recent years the need for biosensors is very high, both in detecting biological samples whose refractive index changes very small. Several ways have been reported to overcome this, using surface plasmon resonance (SPR) technology based on photonic crystal fiber (PCF) will be a good technique in detecting analyte samples [1], for various applications such as in the medical world [2], food safety [3], environment and biochemistry [4]. SPR sensors are widely used in glucose sensing [5], virus detection [6], gas sensing [7], blood type detection [8], environmental sensing [9], food quality measurement [10], telemedicine [11], sensing temperature [12]-[15] and antigen-antibody interactions and other biochemical applications [13].

The technology was first proposed by Ritchie *et al.* in 1950, then Kretschmann and Otto introduced that optical excitation has basically two ways, such as attenuated total reflection (ATR) in a prism-coupler-based structure and diffraction in a lattice in 1968 [14], [15]. Many researchers have used the SPR technique which is applied as a sensor. Furthermore, Nylander and Liedberg introduced the application of attenuated total reflection in the application of SPW in 1983. Prismcoupler-based structures are in large size and large mechanical arrangement process [16]. A remarkable expansion was created after the basic idea of photonic crystal fiber (PCF) was given by Yeh *et al.* in 1978 and discovered by 2D PCF by P. Russel *et al.* in 1992 [17]. So that the incorporation of PCF-based SPR techniques offers advantages that make with micro size and

good performance. PCF is a modern fiber that has air holes around the cladding and core [18], unlike other optical fibers which only consist of a core, cladding, coating, orBraggg lattice fiber [19] PCF has air holes around the core which has many geometric structures reported, PCF is usually composed of fused silica material. However, recently many studies have reported using different materials such as using topas [20], Zeonex [21], SF2 [22], and BK7 glass [23]. Although from research it was reported that PCF with silica material was able to provide relatively high sensitivity, high effective material loss, and low confinement loss. However, PCF with SF2 material has a high confinement loss compared to fused silica [22]. PCF in analyte sensing is usually combined with plasmonic materials to give rise to SPR phenomena such as gold [24], silver [25] titanium oxide (TiO2) [26], silicon nitride (Si3N4) [27], aluminum [28], copper [29], and indium tin oxide (ITO) [30]. PCF-based SPR sensors have advantages over other sensors such as lightweight, microstructure [31], and wide sensing range [32]. Due to the presence of polarized light, the evanescent poles collide with the plasmonic material, creating surface plasmon waves (SPW). SPW depends on the refractive index of the surrounding medium (RI) which depends on the wavelength. For certain RI conditions, the maximum energy of the surface mode polariton (SPP) is transferred, this event is called resonance. So that PCF-based SPR has a fast and good response in detecting analytes [1].

Several studies related to PCF-SPR have been reported, some of which have complex structures and geometries that are difficult to fabricate as reported by Yang *et al.* PCF-SPR has a concave geometric structure that has low confinement loss values and wavelength sensitivity (WS). High that is 10,700 nm/RIU [33], the H-shaped PCF-SPR was also reported by Han *et al.* and it was found that the sensor sensing range was very large and the WS was obtained at 25,900 nm/RIU [34], further research conducted by sakib demonstrated The PCF-SPR is in the form of a slot circuit and it is found that the WS is 16,000 nm/RIU [35]. Rahman *et al.* reported a PCF-SPR with a gold layer surrounding the microchannels having a WS of 25,000 nm/RIU [36]. Shayma *et al.* also investigated PCF-SPR in the form of a Mercedes Benz logo and obtained a WS of 700 nm/RIU [37]. However, most of the PCF-SPR recommended by many researchers have weaknesses in terms of fabrication, and a narrow sensing range that will make the fabrication cost expensive. PCF-SPR which has a simple structure has good performance and is easy to fabricate will make PCF-SPR a sophisticated technology that is effective in exploiting its advantages for detecting analytes. In this paper, we propose Hexagonal two layers of Photonics crystal fiber based on surface plasmon resonance (HT-PCF-SPR) with a simple geometric structure and easy fabrication, HT-PCF-SPR also has good performance in detecting analytes within a certain refractive index range, and good sensor resolution.

2.   METHOD AMD SENSOR GEOMETRY STRUCTURE

The design of the proposed PCF-SPR can be seen in Figure 1. The PCF-SPR has a hexagonal two-layer structure covered by gold plasmonic material, with a thickness of 40 nm. The gold layer is attached to the outside of the cladding and is also plated to the two air holes inside the core to give rise to the SPR phenomenon. In the PCF-SPR design, the holes have a tiered size, and the hole size getting to the center of the PCF has a smaller size. The hole sizes are d1 and d3 with different hole sizes and the distance between holes is d2. This paper also investigates the effect of the size of the air hole on the confinement loss value of the resulting material. The material used in this design is fused silica which can be defined in (1). Geometric structure of air holes and gold material HT-PCF-SPR As shown in Figure 1, size d1=0.46 µm, d2=1.8 µm, d3=0.35 µm and d4=0.4275 µm, meanwhile the thickness of gold is 40 nm. The method used in developing the HT-PCF-SPR is the finite element method (FEM) method with the help of COMSOL Multiphysics 5.6 software. The gold material used is defined as in (2). The analyte sensing system is carried out with an external sensing scheme.
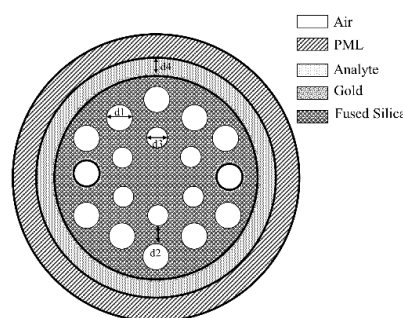

Figure 1. The geometrical structure of the proposed HT-PCF-SPR

Figure 1 shows the proposed geometric structure, the geometric structure of PCF-SPR is hexagonal 2 layers, with a hole size approaching the core having a diameter of d1 and hole size in the outermost layer having a diameter of d2. The distance between the holes is d2. Furthermore, the plasmonic material coats the two holes in the cladding and coats the core structure of the PCF clad. The size of the plasmonic material is 40 nm. The PCF material used in this study is fused silica. The analyte sensing layer is after the gold layer or also known as external sensing. At the end of the layer, a PML boundary layer with a width of 0.70125 µm was applied. Each air hole is arranged at an angle of 30°, 90°, and 150° for the first layer so as to form a hexagonal structure. The same is also done for the second layer of HT-PCF but with a larger air hole size compared to the first layer. Furthermore, in COMSOL the sensing wavelength is set at 750 nm. So that the cross-section is obtained as shown in Figure 2.

3. RESULTS AND DISCUSSION

In this paper, we investigate the hexagonal two-layer (HT-PCF-SPR) PCF-SPR design using the finite element method (FEM) using COMSOL Multiphysics 5.6. The PCF is covered by gold plasmonic material in the cladding and two holes in the core. In this investigation, PCF uses fused silica which can be defined by the sellmeier equation as in (1). Fused silica is a PCF material that is often used, and is reported to have the best performance when compared to other materials such as TOPAS, and Zeonex. The sellmeier equation can be used in defining the fused silica material in the HT-PCF-SPR design. The distribution of the refractive index for silica materials can be seen in (1) [35].

$$n(\lambda) = \sqrt{1 + \frac{0.696\lambda^2}{\lambda^2-0.0047} + \frac{0.408\lambda^2}{\lambda^2-0.014} + \frac{0.897\lambda^2}{\lambda^2-97.934}} \tag{1}$$

Where n is the refractive index of silica for each particular wavelength, Lambda is the wavelength used in PCF-SPR. The plasmonic material used to elicit the SPR effect on the PCF, the plasmonic material used in this study is gold, gold is chemically more stable than the environment but shows a wide resonance peak and this will harm the components. The drude-Lorentz model is used in calculating the dielectric constant of gold which can be shown in (2) [38].

$$\varepsilon_{au} = \varepsilon_{\infty} - \frac{\omega_D^2}{\omega(\omega+j\gamma_D)} - \frac{\Delta\varepsilon\Omega_L^2}{(\omega^2-\Omega_L^2)+j\Gamma_L\omega} \tag{2}$$

With Au being the gold permittivity value, and high-frequency permittivity with a value of 5.9673, then ω is the plasma frequency, where ωD is the dumping frequency and γD is the plasmon frequency which numerically has a value of 31.84π THz and 4227.2π THz and the oscillator power with symbol L = 1300.14π THz, and the spectral width is L = 209.72π THz. PCF that has air holes around the surface will cause loss when I pass through the surface. Confinement loss can be defined as (3) [35].

$$L_c(dB/cm) = \left(\frac{4\pi f}{c}\right) Im(n_{eff}) \times 10^4 \tag{3}$$

Where Lc is the material confinement loss, with a value of 3.14, f = frequency, n_{eff} is the effective refractive index, and c is the speed of light. Meanwhile, wavelength sensitivity can be defined in (4).

$$S_\lambda(nm/RIU) = \frac{\Delta\lambda_{peak}}{\Delta n} \tag{4}$$

Wavelength sensitivity shows how big the shift in the wavelength of the peak loss is for each change in the analyte's refractive index. A large shift for a small change in the refractive index of the analyte will show components that are ultra-sensitive and have high performance in differentiating changes in the refractive index of the analyte. Wavelength sensitivity also shows the difference in peak loss at a certain wavelength divided by the difference in the sensing refractive index. Furthermore, the sensor resolution is mathematically shown by (5) [34].

$$R = \frac{\Delta n_a \times \Delta\lambda_{min}}{\Delta\lambda_{peak}} \tag{5}$$

3.1. Cross-section HT-PCF-SPR

After numerical simulation, the cross-section of HT-PCF-SPR is obtained which is designed as shown in Figure 2. Gold plasmonic material coated in PCF-SPR cladding with a thickness of 40 nm gives rise to the SPR phenomenon as shown in Figure 2(a). Meanwhile, the polarization on the x-axis is shown in Figure 2(b) and the polarization of light on the nucleus that leads to the y-axis is shown in Figure 2(c).
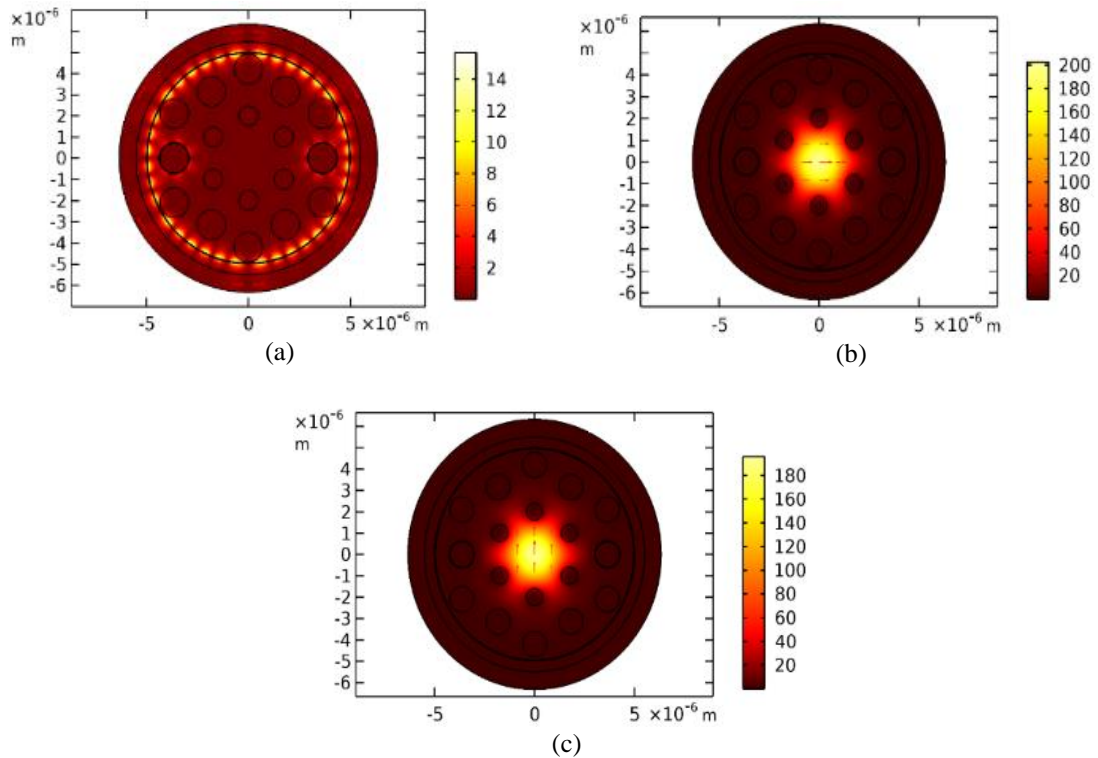

(a)   (b)

(c)

Figure 2. The proposed PCF-SPR cross-section (a) surface plasmon mode, (b) x-polarization, and (c) y-polarization

The cross-section of PCF-SPR is shown in Figure 3. The polarization of light on the x-axis and y-axis is shown. Polarized light around the PCF-SPR surface with a cross-section as shown in Figure 3. This y-axis polarization is then explored to find the effective refractive index for each change in the analyte's refractive index on the component. So, from the imaginary value of the effective refractive index of each analyte for a certain wavelength, it can be found the confinement loss value of the material. The real refractive index and material confinement loss values in this design can be shown in Figure 3. It was found that the analyte refractive index of 1.35 RIU has the largest confinement loss peak. Figure 2(a) shows the cross-section surface plasmonic resonance component.
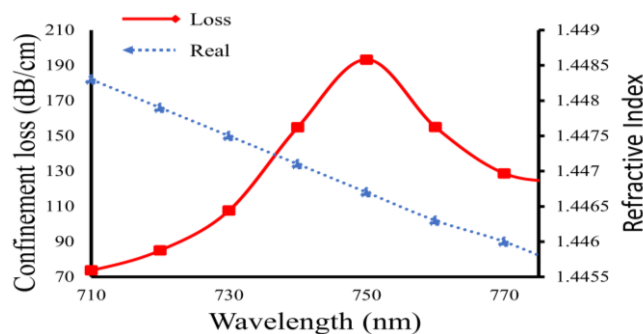

Figure 3. Cross section of HT-PCF-SPR with a thickness of Au 40 nm

3.2. Performance analysis for analytical detection

Furthermore, an analysis is carried out for each PCF-SPR hole distance to obtain the confinement loss shift in Figure 4. The farther the hole distance, the greater the confinement loss. It was found that the Hexagonal two-layer PCF-SPR can detect analytes in the range of 1.34 to 1.37 RIU as obtained in the figure below. The sensitivity of the hexagonal two layers PCF-SPR is 2,000 nm/RIU, every change of 1 RIU experiences a shift in the peak wavelength loss of 2,000 nm. These results show good sensitivity to detect analytes. HT-PCS-SPR can detect analytes with a refractive index of 1.34 to 1.37 RIU in the wavelength range of 730 nm to 810 nm. While the sensor resolution obtained is 6.67×10^{-5}. It is also found that the full width half maximum (FWHM) of the loss is 20 nm. The FWHM measure also shows that the sensor component has high accuracy in detecting the analyte. With the simple structure of HT-PCF-SPR and also showing good performance in detecting analytes, the design of this component can be applied to the biological or biochemical field to detect analytes, or can also be applied to detect healthy cells analytes and cancer cell analytes.
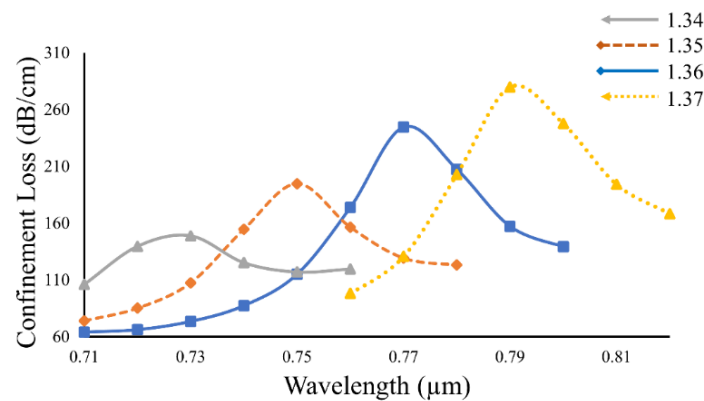
Figure 4. The shift of the confinement loss peak for each different wavelength

3.3. Performance analysis for different hole size distances

Next, the air hole size was analyzed from HT-PCF-SPR, this analysis was shown on hole sizes d1 and d3 in the range of 0.41 µm–0.46 µm and 0.3 µm–0.35 µm, respectively. as shown in Figure 5. The refractive index of the analyte is made the same in this case, namely 1.34 RIU and the peak wavelength of confinement loss is 750 nm. It was found that the larger the size of the air hole in the HT-PCF-SPR design will also give the greater confinement loss of material, it is shown that at a wavelength of 750 nm, the HT-PCF-SPR with sizes d1 and d3 are 0.41 µm and 0.3 µm, respectively. The confinement loss sensor is 191.1 dB/cm, then for sizes, d1 and d3 are 0.42 µm and 0.31 µm, the confinement loss value is 192.1 dB/cm, there is an increase in confinement loss by 1 dB/cm, and so on, the confinement loss value increases with size. the air hole increases. The biggest loss confinement in size 1 is the value of d1 and d3 respectively 0.46 µm and 0.35 µm with a value of further the influence of the size of the air hole on the confinement loss value can be seen in Figure 6.
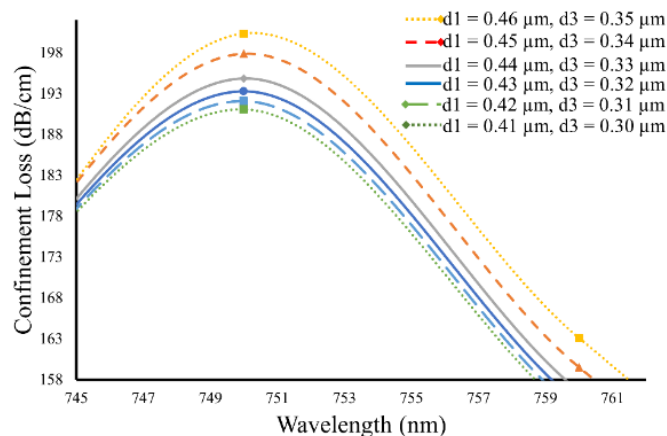

Figure 5. Analysis of HT-PCF-SPR performance on air hole size at 1.35 analyte refractive index
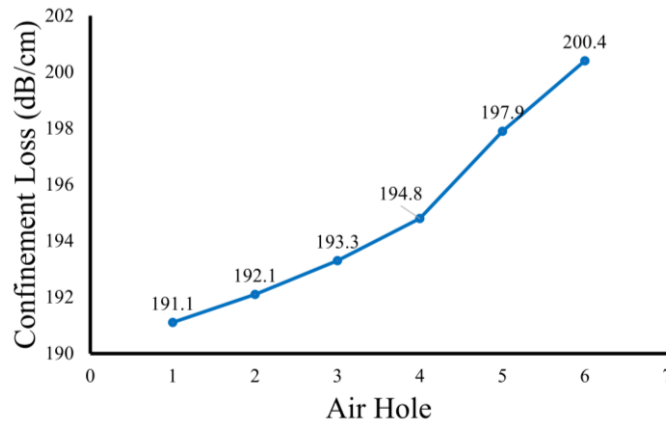
Figure 6. Effect of hole size on component confinement loss

Hole sizes 1, 2, 3, 4, 5, and 6 are each the same variable value according to Figure 5. Figure 6 shows that the larger the air hole in the sensor component gives a larger confinement loss value, and it is obtained that HT-PCF-SPR can detect analytes in the range 1.34–1.37 RIU. This analyte range is evidenced by the presence of polarization to determine the imaginary effective refractive index that will be needed in determining the loss value, this is in accordance with (3). Figure 6 gives an almost linear value between hole size and material loss. Air hole 6 is the size of the largest hole diameter and also shows the most loss value, which is 200.4 dB/cm.

3.4. PCF-SPR performance analysis based on Distance between holes

Furthermore, the effect of the distance between holes was investigated with the loss that occurred in HT-PCF-SPR, in this case, the hole distance was varied by 1.8 μm, 1.9 μm, and 2 μm. This variation is taken to determine how much influence the size of the air hole has on material loss. It can be seen that the smaller the PCF-SPR hole distance, the smaller the component loss value in that range. These results indicate that the HT-PCF-SPR component will have a fairly large material loss value when compared to the components that have been proposed by other researchers. At a wavelength of 770 nm, HT-PCF-SPR with a hole distance of 1.8 μm has a confinement loss value of 227.88 dB/cm, while if the hole distance is increased to 1.9 μm the loss produced by HT-PCF-SPR is only 171.8 dB/cm then when raised to 2 μm the confinement loss is very small, only 130.78 dB/cm. Meanwhile, at a wavelength of 780 nm, all confinement loss values for air hole distances increased, respectively, approaching 104 dB/cm, 88 dB/cm, and 50 dB/cm. so these results indicate that when the HT-PCF-SPR component is fabricated with a 3-dimensional size, each increase in the length of the component will experience a different increase in a loss at a certain air hole distance. This result shows that the peak value of confinement loss occurs at a wavelength of 790 nm, after reaching that wavelength the value of each confinement loss also decreases as shown in Figure 7.
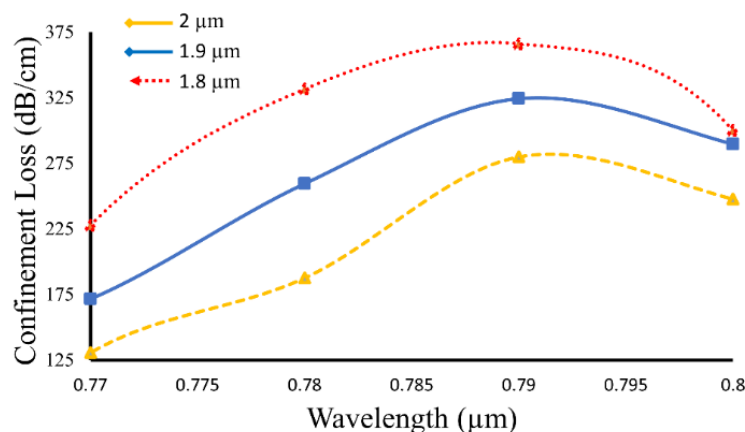

Figure 7. Distribution of HT-PCF-SPR confinement loss value to air hole distance

In Figure 7, the effect of the air hole distance on the confinement loss value is investigated for the same hole size, the difference being the distance between one hole and another. This will also result in the diameter size of the resulting HT-PCF-SPR having a large dimension, getting bigger when the air hole distance is also large. Meanwhile, the gold layer is defined the same for each component, namely 40 nm.

4. CONCLUSION

The HT-PCF-SPR sensor was investigated for different polarization modes as core, cladding, and spp. The plasmonic material used in this paper is gold with a thickness of 40 nm. The HT-PCF-SPR component was designed using the finite element method (FEM) assisted by COMSOL Multiphysics software. The design results found that the HT-PCF-SPR can detect the refractive index in the range of 1.34-1.37 RIU and operate in the wavelength range of 730 nm–810 nm. It was found that the confinement loss component was getting bigger as the air hole size was getting bigger. In detecting the HT-PCF-SPR analyte, which has a sensitivity of 2,000 nm/RIU, the sensor resolution was found to be 6.67×10^{-5} RIU. The sensor component is recommended for sensing in the biological and biochemical fields because it has high sensitivity, and good resolution and the HT-PCF-SPR geometry is simple and easy to fabricate.

REFERENCES

[1]   W. Liu *et al.*, "A square-lattice D-shaped photonic crystal fiber sensor based on SPR to detect analytes with large refractive indexes," *Phys. E Low-Dimensional Syst. Nanostructures*, vol. 138, 2022, doi: 10.1016/j.physe.2021.115106.

[2]   A. Ramola, A. Marwaha, and S. Singh, "Design and investigation of a dedicated PCF SPR biosensor for CANCER exposure employing external sensing," *Appl. Phys. A Mater. Sci. Process.*, vol. 127, no. 9, 2021, doi: 10.1007/s00339-021-04785-2.

[3]   E. K. Akowuah, T. Gorman, H. Ademgil, and S. Haxha, "A highly sensitive photonic crystal fibre (PCF) surface plasmon resonance (SPR) sensor based on a bimetallic structure of gold and silver," in *Proceedings of the 2012 IEEE 4th International Conference on Adaptive Science and Technology, ICAST 2012*, 2012, pp. 121–125, doi: 10.1109/ICASTech.2012.6381078.

[4]   A. Kumar Shakya and S. Singh, "Design of novel Penta core PCF SPR RI sensor based on fusion of IMD and EMD techniques for analysis of water and transformer oil," *Meas. J. Int. Meas. Confed.*, vol. 188, 2022, doi: 10.1016/j.measurement.2021.110513.

[5]   M. E. Rahaman, R. H. Jibon, M. S. Ahsan, F. Ahmed, and I. B. Sohn, "Glucose level measurement using photonic crystal fiber–based plasmonic sensor," *Plasmonics*, vol. 17, no. 1, 2022, doi: 10.1007/s11468-021-01497-4.

[6]   D. Rajeswari and A. A. Revathi, "Highly sensitive SPR-based PCF bio sensor for plasma cell detection in human blood for the detection of early stage cancer," *Optik (Stuttg).*, vol. 258, 2022, doi: 10.1016/j.ijleo.2022.168897.

[7]   R. Senthil, U. Anand, and P. Krishnan, "Hollow-core high-sensitive photonic crystal fiber for liquid-/gas-sensing applications," *Appl. Phys. A Mater. Sci. Process.*, vol. 127, no. 4, 2021, doi: 10.1007/s00339-021-04417-9.

[8]   M. M. A. Eid, M. A. Habib, M. S. Anower, and A. N. Z. Rashed, "Hollow core photonic crystal fiber (PCF)–based optical sensor for blood component detection in terahertz spectrum," *Brazilian J. Phys.*, vol. 51, no. 4, pp. 1017–1025, 2021, doi: 10.1007/s13538-021-00906-7.

[9]   F. A. Mou, M. M. Rahman, M. R. Islam, and M. I. H. Bhuiyan, "Development of a photonic crystal fiber for THz wave guidance and environmental pollutants detection," *Sens. Bio-Sensing Res.*, vol. 29, 2020, doi: 10.1016/j.sbsr.2020.100346.

[10]   A. V. Malinin, A. A. Zanishevskaja, V. V. Tuchin, Y. S. Skibina, and I. Y. Silokhin, "Photonic crystal fibers for food quality analysis," in *Biophotonics: Photonic Solutions for Better Health Care III*, 2012, vol. 8427, p. 842746, doi: 10.1117/12.924096.

[11]   H. Inan, M. Poyraz, F. Inci, M. A. Lifson, M. Baday, B. T. Cunningham, and U. Demirci, "Photonic crystals: emerging biosensors and their promise for point-of-care applications," *Chemical Society Reviews*, vol. 46, no. 2. pp. 366–388, 2017, doi: 10.1039/c6cs00206d.

[12]   S. R. Qutb, A. H. Aly, and W. Sabra, "Salinity and temperature detection for seawater based on a 1D-defective photonic crystal material," *Int. J. Mod. Phys. B*, vol. 35, no. 1, 2021, doi: 10.1142/S0217979221500120.

[13]   D. Irawan, K. Ramadhan, S. Saktioto, and A. Marwin, "Performance comparison of TOPAS chirped fiber Bragg grating sensor with Tanh and Gaussian apodization," *Indonesian Journal of Electrical Engineering and Computer Science (IJEECS),* vol. 26, no. 3, pp. 1477–1485, 2022, doi: 10.11591/ijeecs.v26.i3.pp1477-1485.

[14]   T. Saktioto, K. Ramadhan, Y. Soerbakti, D. Irawan, and Okfalisa, "Apodization sensor performance for TOPAS fiber Bragg grating," *TELKOMNIKA*, vol. 19, no. 6, 2021, doi: 10.12928/telkomnika.v19i6.21669.

[15]   T. Saktioto, K. Ramadhan, Y. Soerbakti, D. Irawan, and Okfalisa, "Integration of chirping and apodization of Topas materials for improving the performance of fiber Bragg grating sensors," in *Journal of Physics: Conference Series*, vol. 2049, no. 1, 2021, doi: 10.1088/1742-6596/2049/1/012001.

[16]   Y. N. Zhang, Y. Zhao, T. Zhou, and Q. Wu, "Applications and developments of on-chip biochemical sensors based on optofluidic photonic crystal cavities," *Lab on a Chip*, vol. 18, no. 1. pp. 57–74, 2018, doi: 10.1039/c7lc00641a.

[17]   R. R. H, "Plasma losses by fast electrons in thin films," *Phys. Rev.*, vol. 106, no. 5, pp. 874–881, 1957.

[18]   B. Liedberg, C. Nylander, and I. Lunström, "Surface plasmon resonance for gas detection and biosensing," *Sensors and Actuators*, vol. 4, no. C, pp. 299–304, 1983, doi: 10.1016/0250-6874(83)85036-7.

[19] J. C. Knight, T. A. Birks, P. S. J. Russell, and D. M. Atkin, "All-silica single-mode optical fiber with photonic crystal cladding: errata," *Opt. Lett.*, vol. 22, no. 7, p. 484, 1997, doi: 10.1364/ol.22.000484.

[20] R. Zhang, J. Teipel, and H. Giessen, "Theoretical design of a liquid-core photonic crystal fiber for supercontinuum generation," *Opt. Express*, vol. 14, no. 15, p. 6800, 2006, doi: 10.1364/oe.14.006800.

[21] C. Martelli, J. Canning, N. Groothoff, and K. Lyytikainen, "Strain and temperature characterization of photonic crystal fiber Bragg gratings," *Opt. Lett.*, vol. 30, no. 14, p. 1785, 2005, doi: 10.1364/ol.30.001785.

[22] B. K. Paul and K. Ahmed, "Highly birefringent TOPAS based single mode photonic crystal fiber with ultra-low material loss for Terahertz applications," *Opt. Fiber Technol.*, vol. 53, 2019, doi: 10.1016/j.yofte.2019.102031.

[23] S. Sen, M. Abdullah-Al-Shafi, A. S. Sikder, M. S. Hossain, and M. M. Azad, "Zeonex based decagonal photonic crystal fiber (D-PCF) in the terahertz (THz) band for chemical sensing applications," *Sens. Bio-Sensing Res.*, vol. 31, 2021, doi: 10.1016/j.sbsr.2020.100393.

[24] F. A. Al-Zahrani and M. A. Kabir, "Ring-core photonic crystal fiber of terahertz orbital angular momentum modes with excellence guiding properties in optical fiber communication," *Photonics*, vol. 8, no. 4, 2021, doi: 10.3390/photonics8040122.

[25] M. E. Rahaman, M. B. Hossain, and H. S. Mondal, "Effect of background materials in photonic crystal fiber sensor," *Opt. Rev.*, vol. 29, no. 1, 2022, doi: 10.1007/s10043-021-00712-1.

[26] C. Liu *et al.*, "The single-polarization filter composed of gold-coated photonic crystal fiber," *Phys. Lett. Sect. A Gen. At. Solid State Phys.*, vol. 383, no. 25, pp. 3200–3206, 2019, doi: 10.1016/j.physleta.2019.07.012.

[27] M. R. Momota and M. R. Hasan, "Hollow-core silver coated photonic crystal fiber plasmonic sensor," *Opt. Mater. (Amst).*, vol. 76, pp. 287–294, 2018, doi: 10.1016/j.optmat.2017.12.049.

[28] Z. Zhang, T. Shen, H. Wu, Y. Feng, and X. Wang, "A temperature sensor based on D-shape photonic crystal fiber coated with Au–TiO2 and Ag–TiO2," *Opt. Quantum Electron.*, vol. 53, no. 12, 2021, doi: 10.1007/s11082-021-03336-6.

[29] X. Chen *et al.*, "High-finesse Fabry-Perot cavities with bidimensional Si3N4 photonic-crystal slabs," *Light Sci. Appl.*, vol. 6, no. 1, 2017, doi: 10.1038/lsa.2016.190.

[30] Q. Liu, Z. Ma, Q. Wu, and W. Wang, "The biochemical sensor based on liquid-core photonic crystal fiber filled with gold, silver and aluminum," *Opt. Laser Technol.*, vol. 130, 2020, doi: 10.1016/j.optlastec.2020.106363.

[31] A. A. Rifat *et al.*, "Copper-graphene-based photonic crystal fiber plasmonic biosensor," *IEEE Photonics J.*, vol. 8, no. 1, 2016, doi: 10.1109/JPHOT.2015.2510632.

[32] S. Mittal, T. Sharma, and M. Tiwari, "Surface plasmon resonance based photonic crystal fiber biosensors: A review," in *Materials Today: Proceedings*, vol. 43, pp. 3071–3074, 2021, doi: 10.1016/j.matpr.2021.01.405.

[33] A. Shafkat, A. N. Z. Rashed, H. M. El-Hageen, and A. M. Alatwi, "The effects of adding different adhesive layers with a microstructure fiber sensor based on surface plasmon resonance: A numerical study," *Plasmonics*, vol. 16, no. 3, pp. 819–832, 2021, doi: 10.1007/s11468-020-01352-y.

[34] W. Luo, J. Meng, X. Li, D. Yi, F. Teng, Y. Wang, and X. Hong, "Long-range surface plasmon resonance sensor based on side-polished D-shaped hexagonal structure photonic crystal fiber with the buffer layer of magnesium fluoride," *J. Phys. D. Appl. Phys.*, vol. 54, no. 50, 2021, doi: 10.1088/1361-6463/ac1dda.

[35] Z. Yang, L. Xia, C. Li, X. Chen, and D. Liu, "A surface plasmon resonance sensor based on concave-shaped photonic crystal fiber for low refractive index detection," *Opt. Commun.*, vol. 430, pp. 195–203, 2019, doi: 10.1016/j.optcom.2018.08.049.

[36] H. Han *et al.*, "A large detection-range plasmonic sensor based on an h-shaped photonic crystal fiber," *Sensors (Switzerland)*, vol. 20, no. 4, 2020, doi: 10.3390/s20041009.

[37] M. N. Sakib *et al.*, "Numerical study of circularly slotted highly sensitive plasmonic biosensor: A novel approach," *Results Phys.*, vol. 17, 2020, doi: 10.1016/j.rinp.2020.103130.

[38] M. T. Rahman, S. Datto, and M. N. Sakib, "Highly sensitive circular slotted gold-coated micro channel photonic crystal fiber based plasmonic biosensor," *OSA Contin.*, vol. 4, no. 6, p. 1808, 2021, doi: 10.1364/osac.425279.

BIOGRAPHIES OF AUTHORS

Dr. Dedi Irawan, M. Sc. 🆔 Ⓖ SC Ⓟ is a lecturer at Physics Education, Dept. of Education of Mathematics and Natural Sciences, Universitas Riau, Pekanbaru, Indonesia. He works on basic and advanced Photonics. He has published many articles and supervised Master's degree and Doctoral degrees since 2015 in Universiti Teknologi Malaysia. Currently research focus on Fiber Bragg Grating sensor (FBG), and Mach-Zehnder Interferometer. Furthermore, he is also doing some research in optoelectronic and optical sensors utilizing FBG, MZI, and directional couplers for medical and agricultural applications. He can be contacted at email: dedi.irawan@lecturer.unri.ac.id.

Khaikal Ramadhan S. Si. 🆔 Ⓖ SC Ⓟ was a student at the University of Riau in 2017 and has finished studying Physics at the University of Riau with a B.Sc. degree in 2021. He interests include applied physics, Photonics, and Optical Fiber for communication and sensor. currently joint research focus in Fiber Bragg grating sensor, MZI, and PCF-SPR. He can be contacted at email: khaikal.ramadhan4946@student.unri.ac.id.

Prof. Dr. Saktioto, S. Si., M. Phil. 🆔 📷 SC Ⓟ is a Senior lecturer at Physics Dept., Faculty of Mathematics and Natural Sciences, Universitas Riau, Pekanbaru, Indonesia. He works on Plasma and Photonics Physics. He has published numbers of article in indexed journal reporting his work in plasma photonic, and it's related with fiber coupler fabrication. He also active doing supervision in Master and Doctoral degree since 2009. Currently his research focus is photonics and plasma industry for communication and biosensors. He can be contacted at email: Saktioto@yahoo.com.

Prof. Dr. Fitmawati, M.Si. 🆔 📷 SC Ⓟ is an active lecturer in biology at the University of Riau. she is active in research and publications and now involved in PCF-SPR research as sensor for biochemical. She is a professor of biology at the University of Riau. She completed her Master and doctoral studies at Institut Pertanian Bogor. She can be contacted at email: fitmawati2008@yahoo.com.

Dwi Hanto, Ph.D. 🆔 📷 SC Ⓟ is a researcher at at Research center of physics National Research and Innovation Agency PUSPIPTEK Indonesia. He actively conducts research and publications related to FBG, Optical Fiber, and PCF-SPR as sensors. He completed his Master and doctoral studies at Universitas Indonesia and Kanazawa University in optoelectronics. He can be contacted by email: dwi.hanto.fisika@gmail.com.

Dr. Bambang Widiyatmoko, M.Eng. 🆔 📷 SC Ⓟ is a senior researcher at Research center of physics National Research and Innovation Agency PUSPIPTEK Indonesia, he has expertise in the field of optical instrumentation. He completed his Master and doctoral studies at Tokyo institute of technology. He focused on research related to FBG, Optical Fiber and PCF-SPR. He can be contacted by email: Widiyatmokobambang@gmail.com.